ChemComm

Non-canonical Lipoproteins with Programmable Assembly and Architecture

Journal:	*ChemComm*
Manuscript ID	CC-COM-05-2020-003271.R2
Article Type:	Communication

COMMUNICATION

Non-canonical Lipoproteins with Programmable Assembly and Architecture

Received 00th January 20xx,
Accepted 00th January 20xx

DOI: 10.1039/x0xx00000x

Md Shahadat Hossain,[†a] Corina Maller,[†a] Yinghui Dai,[b] Shikha Nangi[b,c] and Davoud Mozhdehi[*a,c]

Substrate promiscuity of an acyltransferase is leveraged to synthesize artificial lipoproteins bearing a non-canonical PTM (ncPTM). The non-canonical functionality of these lipoprotein results in a distinctive hysteretic assembly—absent from the canonical lipoproteins—and is used to prepare hybrid multiblock materials with precise and programmable patterns of amphiphilicity. This study demonstrates the promise of expanding the repertoire of PTMs for the development of nanomaterials with unique assembly and function.

Proteins are sequence-defined polymers with applications in healthcare, nano-, and biotechnology.[1,2] The desired function is often encoded in protein sequence by incorporating structural (folded) motifs.[3] However, many proteins contain intrinsically disordered regions (IDRs) without a well-defined structure.[4] The consensus sequences of IDRs are used to design recombinant intrinsically disordered peptide-polymers (IDPPs) for mimicking the structure-function of these biomaterials.[5] Given the lack of well-defined secondary and tertiary interactions in IDPPs, programming their hierarchical assembly is often achieved by designing chimeric sequences using recombinant[6,7] or semisynthetic methods[8] to fuse two regions with different hydrophobicity or structural order, akin to self-assembly of block copolymers. However, the chemical (and functional) design space of chimeric IDPPs produced by genetic engineering is restricted to amino acid-like constituents due to constraints of translational machinery.[9]

To expand the chemical repertoire of protein-based materials, we are inspired by post-translational modifications (PTMs)—the addition of non-proteogenic motifs to proteins after translation.[10] For example, modification of short peptides and

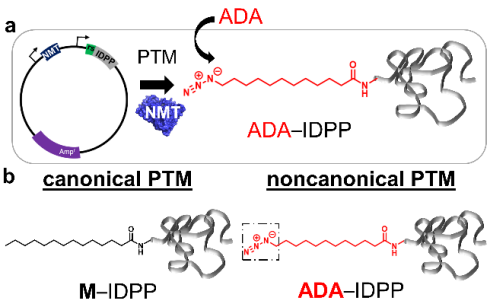

Fig. 1 The substrate promiscuity of biological PTM machinery is used to produce lipoproteins modified with an artificial lipid. a) Our one-pot approach involves co-expression of the NMT enzyme with a protein substrate while supplementing the expression media with an artificial lipid (ADA). The plasmid encodes for 1) the yeast NMT, 2) an elastin-derived IDPP, as a model hydrophilic peptide-polymer, fused to a short peptide substrate of NMT. b) Lipoproteins prepared using canonical PTM (M-IDPP) and non-canonical PTM (ADA-IDPP) are 99.5% identical with only small perturbation in the terminal region of each lipid (boxed structure).

IDPPs with lipids can be used to drive the assembly of hybrid amphiphiles into nanoparticles, given the difference in the hydrophobicity of the polypeptide chain and the lipid group.[11,12] However, the repertoire of lipids in biology is evolutionarily constrained. The canonical lipidation machinery catalyses the transfer of only a few types of lipids (saturated and unsaturated fatty acids, sterols, etc.) to substrate proteins.[13] Though "non-natural" lipidated proteins can be produced via chemoenzymatic methods,[14–16] these approaches are technically challenging, time-consuming, and expensive. Alternatively, biosynthetic routes can address these limitations if their narrow substrate scope is expanded by a combination of metabolic and protein engineering.

As a proof-of-concept, we envisaged using the substrate promiscuity of the PTM machinery to modify proteins with artificial lipids—to form lipoproteins bearing a non-canonical PTM (ncPTM) (Fig. 1). We hypothesized that non-canonical lipoproteins may exhibit unique assembly that is absent from natural analogues, due to the different physicochemical properties of artificial and canonical lipids. Systematic investigation of these analogous lipoproteins will reveal parameters that govern their self-assembly (e.g., lipid shape

[a] *Department of Chemistry, 1-019 Center for Science and Technology, Syracuse University, Syracuse, NY 13244 (USA), E-mail: dmozhdeh@syr.edu.*
[b] *Department of Biomedical and Chemical Engineering, 343 Link Hall, Syracuse University, Syracuse, NY 13244 (USA).*
[c] *BioInspired Syracuse, Syracuse University, Syracuse, NY 13244 (USA)*
† These authors contributed equally to this work.
Electronic Supplementary Information (ESI) available: Materials and methods, supplementary Figures. See DOI: 10.1039/x0xx00000x

and polarity). This fundamental understanding is critical for rational molecular engineering of lipoprotein-based nanocarriers for different biomedical applications. Additionally, artificial lipids bearing bioorthogonal groups (e.g., azide) can be derivatized to form complex hybrid materials. The increased hydrophobicity of these artificial lipids distinguishes their utility from non-canonical amino acids with bioorthogonal side chains,[17] as these lipids can be used to simultaneously couple macromolecules and encode a precise and programmable pattern of amphiphilicity.

In this study, we used the ability of N-myristoyltransferase (NMT) to accept analogues of myristic acid, such as 12-azidododecanoic acid (ADA).[18] ADA has been used to profile myristoylated proteins[19], but the potential of ω-azido fatty acid to develop recombinant nanomaterials with controlled hierarchical assembly is virtually unexplored. We co-expressed i) *S. cerevisiae* NMT with ii) an IDPP fused to a peptide substrate of NMT in *E. coli* (Fig. 1a). The N-terminal glycine of the peptide substrate (GLYASKLFSNL) is the site of lipidation. By adding either myristic acid (M) or ADA to media, canonical (M-IDPP) or non-canonical (ADA-IDPP) lipoproteins were obtained. The concentration of ADA and expression time were adjusted empirically to avoid the misincorporation of endogenous myristic acid (See supplementary information for details). M- and ADA-IDPP only differ in the terminal region of each lipid tail, n-propyl vs. N_3 (Fig. 1b). Compared to M, the azide group increases the polarity of ADA but reduces its packing-efficiency. We, therefore, hypothesized that these differences in physicochemical properties of the lipid tail can lead to divergent assembly pathways for the M-IDPP and ADA-IDPP.

IDPP was derived from the consensus sequence of tropoelastin, $(GXGVP)_{80}$ containing a mixture of valine and alanine (8:2) in X position. IDPPs derived from elastin exhibit lower critical solubility temperature (LCST) phase behaviour[20] and have been used in numerous biomedical and materials science applications.[21,22] We used this LCST phase behaviour to purify IDPP (negative control), M-IDPP, and ADA-IDPP using inverse transition cycling (ITC) after expression (yield of purified proteins = 3-10 mg/L of culture).[23] Mass spectrometry (Fig. S4–5) and labelling with AF_{488}-DBCO (Fig. 2a) confirmed that ADA was efficiently and site-specifically incorporated into desired polypeptides and that the azide remained stable after ITC.

Reverse-phase HPLC was used to quantify the hydrophobicity of each construct by comparing their retention time (t_R). As shown in Fig. 2b, the observed trend—t_R (min) = IDPP (28.8) < ADA-IDPP (30.7) < M-IDPP (31.5)—is consistent with the increased hydrophobicity of M-IDPP compared to ADA-IDPP.

We then investigated whether modification with ADA modulates the liquid-liquid phase separation of IDPP. The turbidity of solutions of IDPP, ADA-IDPP, and M-IDPP (Fig. 3a-c) was monitored while heating or cooling the sample at a rate of 1°C/min. The LCST phase transition resulted in a sharp increase in the turbidity of the solution when the temperature was increased above the transition temperature (T_t). As shown in the partial temperature-composition phase diagram (Fig. 3d, Table S3), both canonical and non-canonical lipids modulated the phase boundaries of parent IDPP. M- and ADA-IDPP exhibited lower T_t compared to the IDPP, and ~75% reduction in the slope of phase-boundaries defined by T_t versus the natural log of the concentration. The observed pseudo-plateau is a possible indicator of the self-assembly of M- and ADA-IDPP at this concentration range. Intriguingly, a closer inspection of the cooling curves revealed a difference in the reversibility of phase transition between the constructs. While the cooling curve of IDPP and M-IDPP, closely matched the heating curve (i.e., smooth change in turbidity), a noticeable shoulder was observed in the cooling curves of ADA-IDPP (at 27–29 °C, marked with an arrow in the Fig. 3b inset). Though no macroscopic aggregates were observed in the cuvettes, we hypothesized that this unexpected behaviour may point to the formation of a new self-assembled structure unique to ADA-IDPP after thermal annealing.

Dynamic light scattering (DLS) and Transmission electron microscopy (TEM) were used to test the hypothesis derived from the turbidimetry. Below T_t, IDPP did not self-assemble (Fig.

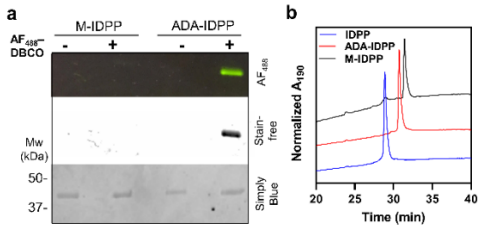

Fig. 2 Molecular characterization confirms the incorporation of ADA. a) Only ADA-IDPP reacts with a fluorophore bearing a dibenzocyclooctyne (DBCO), b) Analytical RP-HPLC confirms the increased hydrophobicity of ADA-IDPP compared to the unmodified IDPP. Since ADA is less hydrophobic compared to myristic acid, ADA-IDPP elutes earlier than M-IDPP.

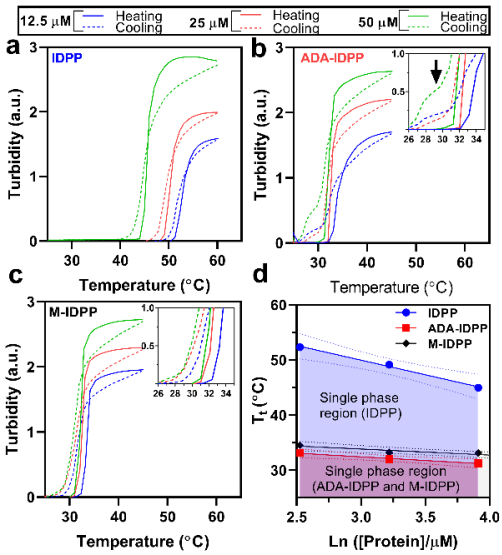

Fig. 3 Temperature-programmed turbidimetry was used to monitor the LCST phase transition of IDPP (a), ADA-IDPP (b), and M-IDPP (c). d) The partial phase diagram for the three constructs, showing the boundaries between the single- and the two-phase region. The dashed lines represent the 90% confidence interval of the line fitted to observed Tt, Table S3. IDPP exhibits a reversible LCST phase transition, characterized by a sharp increase in the turbidity of the solution above T_t and sharp concentration dependence of T_t. Modification with M or ADA modulates IDPP phase behavior. Only ADA-IDPP exhibits a unique "shoulder" in the turbidity profiles during the cooling cycle (inset in b), suggesting the formation of new structures during thermal annealing.

4a) as the hydrodynamic radius (R_h = 6.8 ± 0.2 nm) matched the expected size for the unimer of a coiled protein.[24] The increased R_h of M-IDPP (36.9 ± 0.2 nm) and ADA-IDPP (31.9 ± 0.3 nm) confirms the self-assembly of these constructs (Fig. 4a). TEM confirmed that M-IDPP (Fig. S6a) and ADA-IDPP (Fig. S6b) form similar spherical micelles below T_t, thus conclusively proving that ncPTM can drive the assembly of the recombinant lipoprotein into micelles despite significant differences in the hydrophobicity of the lipid tails ($\Delta \log P_{ADA-M}$ = -0.4).

The hydrodynamic size remained unchanged below the T_t of each construct (Fig. S7). Above LCST, DLS indicated the formation of large (> μm size) polymer-rich coacervates. When the temperature was lowered to 20°C (below T_t), to mimic the effect of thermal annealing, only ADA-IDPP exhibited non-equilibrium (hysteretic) increase in the hydrodynamic size while the size of IDPP and M-IDPP were indistinguishable before and after thermal annealing (Fig. 4b, and S8). This data indicates that the pathway-dependent differences in the phase behaviour of two lipoproteins originate from the changes in the size or morphology of ADA-IDPP assemblies after thermal annealing. We also ruled out that the hysteresis is due to the decomposition of ADA, as the aliphatic azide remained accessible to synthetic elaboration after thermal annealing (Fig. S9).

TEM confirmed that after thermal annealing, ADA-IDPP spherical micelles transitioned to form long fibers (Fig. 5a, diameter 32.9 ± 4 nm, with a length extending over a few microns). Importantly, this observation confirms that minuscule structural perturbations in the terminal fragments of lipid lead to divergent energy landscapes for these lipoproteins, thus encoding the observed hysteretic transition in nano- and meso-scale assembly of ADA-IDPP. Though the assembly of small amphiphilic molecules is very sensitive to structural perturbation, the divergence between the assembly of M- and ADA-IDPP is surprising, considering the highly asymmetric nature of these lipoproteins. Encoding non-equilibrium phase behaviour in IDPPs is an emergent frontier in biomacromolecular engineering and often requires significant alteration to the sequence of polypeptide[25,26] or fusion of domains with defined secondary structure.[27,28] To the best of our knowledge, encoding hysteresis using subtle molecular perturbations is unprecedented in the literature. Recently, an intriguing morphological transition of azide-decorated polymersomes is also reported.[29] Based on this report, we propose that the interaction of strategically placed organic azides with water may influence the properties of the hydration layer surrounding these amphiphilic molecules. Given the widespread application of azides in bioconjugation and metabolic labelling, additional studies are warranted to probe the generality of this concept and its underlying mechanism.

Incorporation of non-canonical lipids with reactive moieties into proteins ushers new opportunities in material design. We envisioned using the reactivity of the azide group to couple two lipoproteins with a precise pattern of amphiphilicity. ADA-IDPP was reacted with a telechelic alkyne (dipropargyl ether) to produce a lipoprotein with bolaamphiphile architecture (BMT-$IDPP_2$) in which the hydrophobic lipid is flanked by two thermally responsive protein domains (Fig. S10-S11). The synthesis of such sequence-defined and monodisperse giant bolaamphiphiles (M_n =72 kDa, PDI=1) is not possible with canonical lipids, as they lack reactive functional groups at both termini.

The self-assembly (Fig. 5b) and phase behaviour (Fig. S12) of BMT-$IDPP_2$ was distinctively different from the ADA-IDPP, highlighting the importance of programmable amphiphilic regions accessible through ncPTM. Below LCST, BMT-$IDPP_2$ self-assembled into 14.1 ± 3.0 nm nanoparticles (Fig. S13), which reversibly transitioned into bottle-brush structures, above LCST (Fig. 5b). These bottle-brush structures contain a thinner core (7.7 ± 1.6 nm), consistent with the size of dimerized lipid domain and 70-80 nm corona (Fig. S14). This programmable assembly was unique to the bolaamphiphile architecture as the control construct, prepared from the reaction of ADA-IDPP with propargyl alcohol, only formed small particles with an average diameter of 6.4 ± 0.2 nm (Fig. S15).

Finally, we developed an *in-silico* model to explain the differences in the assembly of M- and ADA-IDPP. Since 99.5% of two lipoproteins are identical, we confined our atomistic simulations to the N-terminal amphiphilic region (lipid–recognition sequence peptide). Using all-atom molecular dynamics simulations, we captured the differences in the macromolecular assembly of M–peptide, and ADA–peptide. As shown in Fig. 6, M–peptides aggregate via the hydrophobic interactions of the myristoyl chains (green) that form a micellar core while the peptides (purple) form the shell (Fig. 6a). In contrast, in ADA–peptide assembly (Fig. 6b), the polar azide groups (blue) are hydrophilic and remain solvent-exposed, preventing efficient packing and formation of a lipid core. The ADA–peptide aggregate has a consistently higher radius of

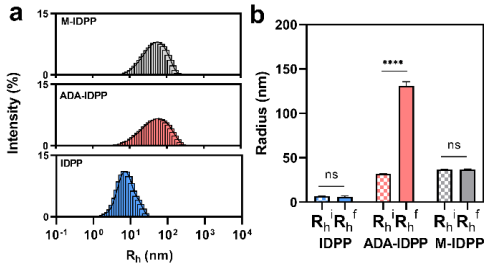

Fig. 4 DLS characterization of the assembly of IDPP, M- and ADA-IDPP. a) IDPP does not self-assemble in solution while ADA-IDPP and M-IDPP form micelles with similar R_h at 20°C < T_t. b) Unlike IDPP and M-IDPP, the hydrodynamic size of ADA-IDPP irreversibly increases after thermal annealing suggesting a change in the assembly state due to physicochemical properties of ADA. mean ± SD (n=3). Two-way Analysis of Variance, ****: p-value <0.0001.

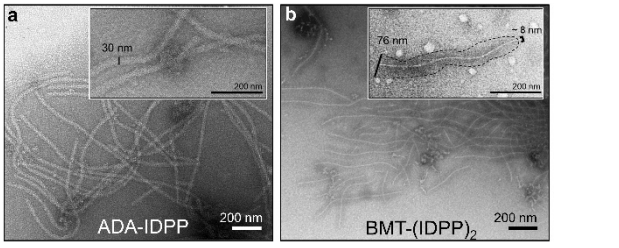

Fig. 5 TEM of ADA-IDPP after thermal annealing. a) ADA-IDPP forms elongated fibers with an average width of 32.9 ± 4.0 nm (n = 80). b) BMT-$IDPP_2$ forms bottle-brush structures with noticeably thinner cores, the average width of 7.7 ± 1.6 nm (n = 50). mean ± SD. See Fig. S14 for the size distribution histograms.

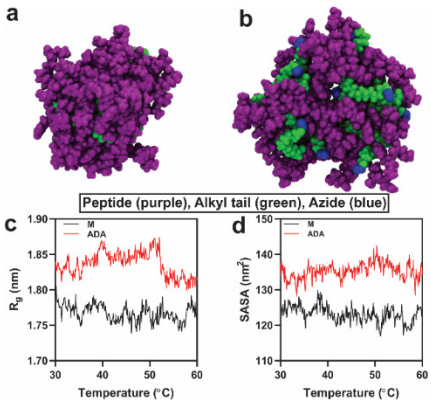

Fig. 6 *In silico* assembly of M–peptide, and ADA–peptide using all-atom molecular dynamics simulations. a) Snapshots of 15 M–peptide molecules showing core-shell structure with myristoyl chains in the core and peptides forming the shell at 40°C. b) Snapshot of 15 ADA–peptide aggregate with ADA chains and terminal azide on the surface of aggregate along with the peptides at 40°C. c, d) The variation in the radius of gyration (R_g), and the solvent accessible surface area (SASA) of the M–peptide (black) and ADA–peptide (red) aggregates over 30–60 °C.

gyration (R_g) and solvent accessible surface area (SASA) compared to M–peptide aggregate (Fig. 6c,d) over the 30–60 °C. The difference in packing efficiency is supported experimentally by the observed critical assembly concentration for ADA-IDPP (18 μM) and M-IDPP (2 μM), Fig. S16. We propose that pathway-dependent differences between the assembly of M- and ADA-IDPP stem from the stability and dynamics of hydrophobic cores (Fig. S17). Though both lipoproteins form similar assemblies at low temperatures, the hydrophobic core of ADA-IDPP is more dynamic, lowering the energy barrier for the rearrangement of the IDPP chains at elevated temperatures.

The well-documented substrate-promiscuity of lipidation machinery has been extensively leveraged in the field of chemical biology.[30–32] We applied these strategies to design novel lipoproteins with emergent material properties such as stimuli-responsive shape-shifting nanomorphology. We foresee several opportunities for the design of dynamic nano-biomaterials in this untapped chemical design space. For example, the programmable morphological change from nanoparticles to fibers can be used to simultaneously release encapsulated cargo and provide a scaffold for cell-adhesion and growth. Non-canonical lipids can also be used as chemical handles for structural elaboration and synthesis of hybrid materials with unique and precise amphiphilic pattern. These hybrid systems can be programmed to assemble into complex 2D and 3D morphologies to form materials with unique optical and mechanical properties.

This research was supported by a start-up grant from Syracuse University (to D.M.), partial support from the National Science Foundation under Grant No. CHE-1659775 (REU) and CBET-1453312 (to S.N.).

Conflicts of interest

There are no conflicts to declare.

Notes and references

1 Y. Liang, L. Li, R. A. Scott and K. L. Kiick, Macromolecules, 2017, 50, 483–502.
2 A. P. Blum, J. K. Kammeyer, A. M. Rush, C. E. Callmann, M. E. Hahn and N. C. Gianneschi, J. Am. Chem. Soc., 2015, 137, 2140–2154.
3 Y. Wang, P. Katyal and J. K. Montclare, Adv. Healthc. Mater., 2019, 8, 1801374.
4 R. A. Metzler, F. Barthelat and J. J. Wilker, Adv. Funct. Mater., 2019, 29, 1805734.
5 Y. J. Yang, A. L. Holmberg and B. D. Olsen, Annu. Rev. Chem. Biomol. Eng., 2017, 8, 549–575.
6 M. B. Van Eldijk, J. C. Y. Wang, I. J. Minten, C. Li, A. Zlotnick, R. J. M. Nolte, J. J. L. M. Cornelissen and J. C. M. Van Hest, J. Am. Chem. Soc., 2012, 134, 18506–18509.
7 S. H. Klass, M. J. Smith, T. A. Fiala, J. P. Lee, A. O. Omole, B.-G. Han, K. H. Downing, S. Kumar and M. B. Francis, J. Am. Chem. Soc., 2019, 141, 4291–4299.
8 T. Luo and K. L. Kiick, J. Am. Chem. Soc., 2015, 137, 15362–15365.
9 A. Hochkoeppler, Biotechnol. Lett., 2013, 35, 1971–1981.
10 K. W. Barber and J. Rinehart, Nat. Chem. Biol., 2018, 14, 188–192.
11 T.-H. Ku, S. Sahu, N. M. Kosa, K. M. Pham, M. D. Burkart and N. C. Gianneschi, J. Am. Chem. Soc., 2014, 136, 17378–17381.
12 K. M. Luginbuhl, D. Mozhdehi, M. Dzuricky, P. Yousefpour, F. C. Huang, N. R. Mayne, K. L. Buehne and A. Chilkoti, Angew. Chem. Int. Ed., 2017, 56, 13979–13984.
13 T. Mejuch and H. Waldmann, Bioconjug. Chem., 2016, 27, 1771–1783.
14 J. M. Antos, G. M. Miller, G. M. Grotenbreg and H. L. Ploegh, J. Am. Chem. Soc., 2008, 130, 16338–16343.
15 S. W. A. Reulen, W. W. T. Brusselaars, S. Langereis, W. J. M. Mulder, M. Breurken and M. Merkx, Bioconjug. Chem., 2007, 18, 590–596.
16 M. Takahara, R. Wakabayashi, N. Fujimoto, K. Minamihata, M. Goto and N. Kamiya, Chem. - A Eur. J., 2019, 25, 7315–7321.
17 R. L. M. Teeuwen, S. S. van Berkel, T. H. H. van Dulmen, S. Schoffelen, S. a Meeuwissen, H. Zuilhof, F. a de Wolf and J. C. M. van Hest, Chem. Commun., 2009, 7345, 4022.
18 B. Devadas, T. Lu, A. Katoh, N. S. Kishore, A. C. Wade, P. P. Mehta, D. A. Rudnick, M. L. Bryant, S. P. Adams, Q. Li, G. W. Gokelp and J. I. Gordon, J. Biol. Chem., 1992, 267, 7224–7239.
19 E. Thinon, R. A. Serwa, M. Broncel, J. A. Brannigan, U. Brassat, M. H. Wright, W. P. Heal, A. J. Wilkinson, D. J. Mann and E. W. Tate, Nat. Commun., 2014, 5, 4919.
20 F. C. M. Smits, B. C. Buddingh, M. B. van Eldijk and J. C. M. van Hest, Macromol. Biosci., 2015, 15, 36–51.
21 G. Qin, M. J. Glassman, C. N. Lam, D. Chang, E. Schaible, A. Hexemer and B. D. Olsen, Adv. Funct. Mater., 2015, 25, 729–738.
22 Z. Li, D. R. Tyrpak, C. L. Lien and J. A. MacKay, Adv. Biosyst., 2018, 2, 1800112.
23 D. E. Meyer and A. Chilkoti, Nat. Biotechnol., 1999, 17, 1112–1115.
24 S. Fluegel, K. Fischer, J. R. McDaniel, A. Chilkoti and M. Schmidt, Biomacromolecules, 2010, 11, 3216–3218.
25 M. J. Glassman and B. D. Olsen, Biomacromolecules, 2015, 16, 3762–3773.
26 F. G. Quiroz, N. K. Li, S. Roberts, P. Weber, M. Dzuricky, I. Weitzhandler, Y. G. Yingling and A. Chilkoti, Sci. Adv., 2019, 5, 1–12.
27 S. Roberts, T. S. Harmon, J. L. Schaal, V. Miao, K. (Jonathan) Li, A. Hunt, Y. Wen, T. G. Oas, J. H. Collier, R. V. Pappu and A. Chilkoti, Nat. Mater., 2018, 17, 1154–1163.
28 D. Mozhdehi, K. M. Luginbuhl, J. R. Simon, M. Dzuricky, R. Berger, H. S. Varol, F. C. Huang, K. L. Buehne, N. R. Mayne, I. Weitzhandler, M. Bonn, S. H. Parekh and A. Chilkoti, Nat. Chem., 2018, 10, 496–505.
29 H. Che, L. N. J. de Windt, J. Zhu, I. A. B. Pijpers, A. F. Mason, L. K. E. A. Abdelmohsen and J. C. M. van Hest, Chem. Commun., 2020, 56, 2127–2130.
30 D. A. Ciulla, A. G. Wagner, X. Liu, C. L. Cooper, M. T. Jorgensen, C. Wang, P. Goyal, N. K. Banavali, J. L. Pezzullo, J.-L. Giner and B. P. Callahan, Chem. Commun., 2019, 55, 1829–1832.
31 K. N. Chuh, A. R. Batt and M. R. Pratt, Cell Chem. Biol., 2016, 23, 86–107.
32 X. Zhang, Z. Xu, D. S. Moumin, D. A. Ciulla, T. S. Owen, R. A. Mancusi, J.-L. Giner, C. Wang and B. P. Callahan, Bioconjug. Chem., 2019, 30, 2799–2804.